Comparison of Current Carrying Capacities and Investment Costs of Directly Buried HVDC Cable and GIL Transmission Systems

Constantin Balzer, M.Sc., Technical University of Darmstadt, constantin.balzer@tu-darmstadt.de
Dipl.-Ing. Martin Hallas, Technical University of Darmstadt, martin.hallas@tu-darmstadt.de
Prof. Volker Hinrichsen, Technical University of Darmstadt, volker.hinrichsen@ tu-darmstadt.de
Prof. Claus Neumann, Technical University of Darmstadt, neumann@hst.tu-darmstadt.de
Dr.-Ing. Hermann Koch, DrKochConsulting, Erlangen, hermann.koch@drkochconsulting.com

Abstract

HVDC underground transmission is of high interest for future grid extension. Generally, directly buried DC cables and DC GIL are possible solutions, and both of them represent new technologies. This paper takes a first step in comparing their current carrying capabilities and investment costs. In order to do so, the ampacity ratings are first calculated for homogenous bedding properties with the help of analytical formulas and a numerical model. This serves as a validation of the model and gives important insights of the differences between the two technologies. In a next step, the ampacity ratings are derived under the influence of realistic constraints, such as the inclusion of drying out of the soil, variations of the backfill material or environmental demands into the calculations. Based on the derived ampacity ratings, the investment costs are assessed, considering a large variation of major cost factors. For two different scenarios, i.e. a transmission capacity of 2.5 GW and 5 GW, the relative project costs are compared.

1 Motivation

Regarding the underground transmission of electrical power by high voltage direct current (HVDC), two different options can be chosen: Since the beginning of HVDC power transmission, underground cables have been used – oil-paper insulated in the beginning, but most recently insulated by cross-linked polyethylene (XLPE). Highest voltage levels are 550 kV (640 kV) [1]. However, since 2019, HVDC power transmission by gas-insulated lines (GIL) is investigated in a large scale field test at the Technical University of Darmstadt [2]. In this case, the main insulation medium is not a solid (as it is in cables), but gas that is contained under high pressure inside a coaxial geometry, consisting of an inner conductor supported by insulators and an outer aluminium tube.

Compared to HVAC systems, for which a detailed comparison of the two technologies GIL and cables has been drawn [3], no such evaluation has been conducted for HVDC systems so far. With this contribution, a first step towards an impartial comparison is embarked.

In principle, a comparison between technologies should include the cost impact of investment, operation and disposal as well as an evaluation of environmental impacts and reliability during operation. One key aspect among the aforementioned factors is the current carrying capacity (equally called the ampacity rating) of the corridor, and this contribution focuses on comparing the ampacity rating of HVDC cables and HVDC-GILs.

In order to do so, the relevant input parameters, i.e. the geometries of the cable or GIL and the bedding as well as the thermal and electric parameters of the implied materials, will be clarified in chapter 2.

In chapter 3, the stationary ampacity rating is derived for homogenous bedding characteristics, using analytical formulas as well as numerical solutions. On the one hand side, this serves as a validation for the numerical models, on the other hand, this gives a good overview about the important factors of influence on the ampacity rating as well as the general differences between the two technologies.

In the following chapter 4, the changes in ampacity ratings under realistic assumptions (such as the drying out of the soil or lower maximum temperatures inside the beddings due to environmental regulations) are studied. And finally, chapter 5 compares the investment costs of the two technologies for an installed transmission capacity of 2.5 GW and 5 GW, presented for a wide range of cost factors.

2 Input parameters

First of all, the input parameters of the simulation must be clarified in order to ensure transparency with respect to the results. This includes the studied geometries as well as the material parameters.

2.1 Geometries of the cable and GIL

In the following, a short overview of the studied geometries of the cable and the gas-insulated line is given. The values are derived from existing technologies, whereas the differences between the different manufacturers are negligible to the results. With regard to the cable system, a typical example of a DC onshore cable with $U_m = 550$ kV and a nominal cross-section of the copper conductor of 2500 mm² will be considered. Concerning the GIL, a prototype with $U_m = 550$ kV will be examined, whose nominal cross section of the hollow aluminium conductor is about 8000 mm². Each system is considered bipolar, i.e. consisting of two poles without a metallic return conductor. The geometries of the cable and GIL are shown in **Figure 1**, the values of the involved radii are given in **Table 1**.

License: CC-BY-NC-ND 4.0 International - Creative Commons, Attribution, NonCommercial, NoDerivatives

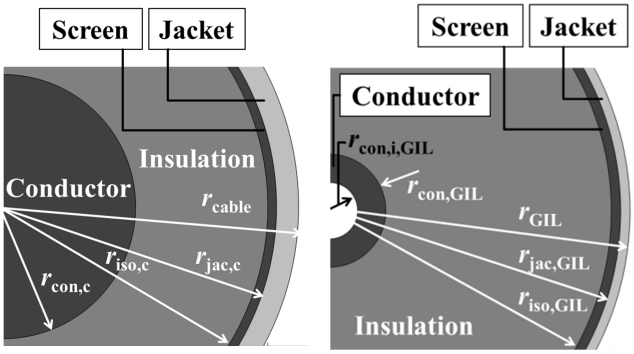

Figure 1 Cross section of an HVDC cable (left) and HVDC-GIL (right) with the parameters of dimension. The scaling is different for the two images.

Table 1 Geometry parameters of the cable and the GIL according to Figure 1

Variable	Cable	GIL
$r_{con,i}$ in mm	-	30
r_{con} in mm	30	60
r_{iso} in mm	60	300
r_{jac} in mm	62	310
r_{cable} or r_{GIL} in mm	67	320

2.2 Geometry of the bedding

Regarding the bedding, three different components must be distinguished: First of all, high voltage cables and GILs are mostly bedded inside thermally stabilized bedding material. This can be temporarily flowable backfill material (as it is recommended for the GIL with respect to mechanical stresses) or sands with a grain size distribution adopted to assure certain levels of heat conductivity under dried-out conditions. This is currently considered for DC cable projects in Germany. Secondly, the upper part of the trench is refilled with a mixture of different on-site soils, of which coarse grains have been removed, and which are frequently compacted. And finally, there is the natural soil which is – apart from a possible compaction due to the construction work on the route – considered as "undisturbed". A cross section of a trench for cables and GILs, including the three named bedding materials, is given in **Figure 2**.

In order to compare the two technologies despite their different geometries, the relative parameters of the trench dimensions that are indicated in Figure 2 have been set as specified in **Table 2**.

Table 2 Relative Geometry parameters of the trench according to Figure 2

Variable	Value
y_0 in m	-1.35
d in m	0.6
$s_1 = s_2$ in m	0.2
s_3 in m	0.6

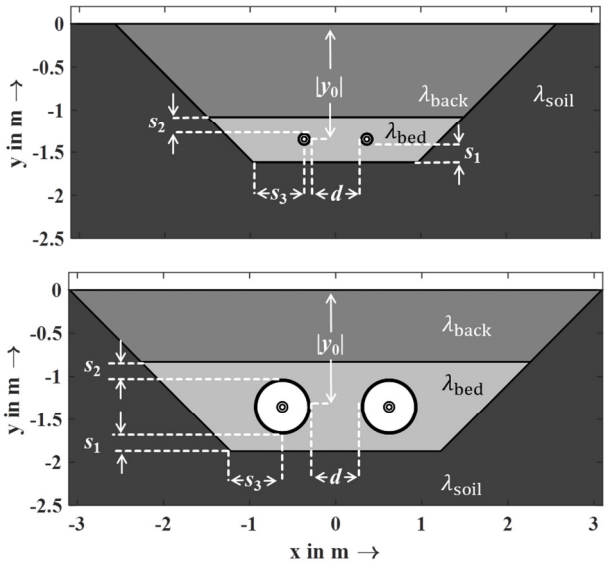

Figure 2 Cross section of a trench for HVDC cables (top) and HVDC-GILs (bottom) with the parameters of dimension. The thermally stabilized bedding material is drawn in light grey, the backfill material in grey and the natural soil in dark grey.

The angle of the trench side is set to 45°. Comparing the volumes of the bedding materials for the parameters of Table 2, **Table 3** gives the resulting numbers.

Table 3 Volumes per unit length for the trenches from Figure 2

	Cable	GIL
Volume of specialized bedding material per meter of length	1.3 m^3	3.0 m^3
Volume of backfill material per meter of length	4.4 m^3	4.4 m^3

2.3 Material properties

Ampacity calculations must take into account the electrical characteristics for the conducting materials as well as the thermal characteristics of all components. The applied values are given in **Table 4** (electrical specifications) and **Table 5** (thermal properties). All thermal properties in Table 5 are considered to be constant with temperature.

Table 4 Electric parameters for the conductor materials

	$R'_{20°C}$ in $\frac{\Omega}{m}$	α in $\frac{1}{K}$
Cable (copper)	$7.2 \cdot 10^{-6}$	$3.93 \cdot 10^{-3}$
GIL (aluminium)	$3.5 \cdot 10^{-6}$	$4.03 \cdot 10^{-3}$

Where:

$R'_{20°C}$: Electric resistivity per unit length of the conductor at 20 °C in $V \cdot A^{-1} \cdot m^{-1}$

α: Temperature coefficient of the conductor's resistivity in K^{-1}

Table 5 Thermal parameters for the materials

	λ in $\frac{\mathrm{W}}{\mathrm{m \cdot K}}$	ρ in $\frac{\mathrm{kg}}{\mathrm{m^3}}$	c_p in $\frac{\mathrm{J}}{\mathrm{kg \cdot K}}$
Aluminium	238	2700	900
Copper	400	8960	385
XLPE	0.3	900	2400
HD-PE	0.4	950	2400
Bedding Materials	Given in the following chapters		

Where:

λ: Thermal conductivity in $\mathrm{W \cdot m^{-1} \cdot K^{-1}}$

ρ: Density in $\mathrm{kg \cdot m^{-3}}$

c_p: Specific heat capacity under constant pressure in $\mathrm{J \cdot kg^{-1} \cdot K^{-1}}$

3 Transmission capacity in the case of a homogenous bedding

For a start, the maximum admissible current for the systems shown in Figure 2 under a time-invariant load will be calculated. In general, this is done in three steps:

1. Calculation of the electric losses per unit length
2. Determination of the thermal resistances of the cable and the GIL, respectively
3. Determination of the thermal resistance of the bedding as well as the thermal interference between the poles

Once the losses per unit length and the involved thermal resistances have been determined, the analogy between the thermal Fourier's law and the Ohmic law can be used to describe the temperature difference between the pole conductor and the reference temperature (i.e. the temperature in laying depths of the poles without the influence of the injected heat):

$$\mathrm{d}T_\mathrm{con} = R_\mathrm{th,sys} \cdot P'_\mathrm{max}(I) + \mathrm{d}T_\mathrm{ad} \tag{1}$$

Where:

$\mathrm{d}T_\mathrm{con}$: Temperature difference between the conductor and the reference temperature in K

$R_\mathrm{th,sys}$: Thermal resistance of the system in $\mathrm{m \cdot K \cdot W^{-1}}$

$P'_\mathrm{max}(I)$: Current dependent conductor losses at maximum operating temperature in $\mathrm{W \cdot m^{-1}}$

$\mathrm{d}T_\mathrm{ad}$: Temperature rise due to the adjacent pole in K

By regrouping equation (1) and inserting the quadratic relation between the conductor losses and the current, the maximum current I_max can be derived as:

$$I_\mathrm{max} = \sqrt{\frac{\mathrm{d}T_\mathrm{max} - \mathrm{d}T_\mathrm{ad}}{R_\mathrm{th,sys} \cdot R'_\mathrm{max}}} \tag{2}$$

Where:

$\mathrm{d}T_\mathrm{max}$: Maximum temperature drop between the conductor and the reference temperature in K

I_max: Maximum conductor current in A

R'_max: Electric resistance per unit length of the conductor at maximum temperature in $\mathrm{V \cdot A^{-1} \cdot m^{-1}}$

In the following, the thermal conductivity of the bedding is assumed to be homogenous and temperature independent. Hence, the differences in thermal properties of the types of beddings as well as a possible soil drying out will be neglected, so that:

$$\lambda_\mathrm{bed} = \lambda_\mathrm{back} = \lambda_\mathrm{soil} = 1 \frac{\mathrm{W}}{\mathrm{m \cdot K}} = \mathrm{const.} \tag{3}$$

Where:

$\lambda_\mathrm{bed}, \lambda_\mathrm{back}, \lambda_\mathrm{soil}$: Thermal conductivities of the specialized bedding, the backfill material and the natural soil in $\mathrm{W \cdot m^{-1} \cdot K^{-1}}$

This rough approximation is useful under two perspectives: First of all, it substantially facilitates the analytical calculation of $\mathrm{d}T_\mathrm{ad}$ and $R_\mathrm{th,sys}$ in equation (2), and therefore making the validation of the numerical results more transparent. Secondly, by reducing the complexity of the bedding, the focus is on the comparison of the two technologies only. The influence of the bedding materials on the ampacity ratings will be further evaluated in chapter 4.

3.1 Calculation of losses

As DC-systems are considered, no induced currents are present. Hence, the losses in the screen or the enclosure are zero, and the conductor losses are determined by:

$$P'_\mathrm{max}(I_\mathrm{max}) = R'_\mathrm{max} \cdot I^2_\mathrm{max} \tag{4}$$

With:

$$R'_\mathrm{max} = R'_{20°\mathrm{C}} \cdot [1 + \alpha \cdot (T_\mathrm{max} - 273\ \mathrm{K})] \tag{5}$$

Where:

T_max: Maximum conductor temperature in K

Inserting $T_\mathrm{max} = 343$ K for the cable or $T_\mathrm{max} = 378$ K for the GIL as well as the values from Table 4 leads to:

$$P'_\mathrm{max,cab}(I_\mathrm{max}) = 8.61 \cdot 10^{-6} \frac{\Omega}{\mathrm{m}} \cdot I^2_\mathrm{max} \tag{6}$$

$$P'_\mathrm{max,GIL}(I_\mathrm{max}) = 4.70 \cdot 10^{-6} \frac{\Omega}{\mathrm{m}} \cdot I^2_\mathrm{max} \tag{7}$$

Hence, due to the larger cross section of the conductor of the GIL, it is:

$$\frac{P'_\mathrm{max,GIL}(I_\mathrm{max})}{P'_\mathrm{max,cab}(I_\mathrm{max})} = 0.55 \tag{8}$$

This means that, given the same current, the GIL conductor causes approximately half the losses compared to the cable conductor.

3.2 Thermal resistance of the cable

As it is justified to neglect the thermal resistances of the screen as well as bedding layers, the thermal resistance of the cable is the sum of the thermal resistance of the insulation and the outer jacket:

$$R_\mathrm{th,cab} = R_\mathrm{th,iso,c} + R_\mathrm{th,jac,c} \tag{9}$$

Where:

$R_\mathrm{th,cab}, R_\mathrm{th,iso,c}, R_\mathrm{th,jac,c}$: Thermal resistances of the cable, the cable insulation and the outer jacket of the cable, in $\mathrm{K \cdot m \cdot W^{-1}}$

As the heat is exclusively transferred by conduction, it is:

$$R_{\mathrm{th,iso,c}} = \frac{1}{2\pi\cdot\lambda_{\mathrm{XLPE}}}\cdot\ln\left(\frac{r_{\mathrm{iso,c}}}{r_{\mathrm{con,c}}}\right) = 0.368\,\frac{\mathrm{K\cdot m}}{\mathrm{W}} \tag{10}$$

$$R_{\mathrm{th,jac,c}} = \frac{1}{2\pi\cdot\lambda_{\mathrm{HDPE}}}\cdot\ln\left(\frac{r_{\mathrm{cable}}}{r_{\mathrm{jac,c}}}\right) = 0.031\,\frac{\mathrm{K\cdot m}}{\mathrm{W}} \tag{11}$$

So that:

$$R_{\mathrm{th,c}} \approx 0.40\,\frac{\mathrm{K\cdot m}}{\mathrm{W}} \tag{12}$$

3.3 Thermal resistance of the GIL

With respect to the internal thermal resistance of the GIL, equation (9) is still valid if the corresponding thermal resistances of the GIL are inserted. However, as the heat between the conductor and the enclosure is transferred via convection as well as radiation, the calculation of $R_{\mathrm{th,iso,GIL}}$ has to take these two mechanisms into account.

3.3.1 Heat transfer by radiation

The heat flux per unit length between two grey bodies, denoted as "a" and "b", of the same emissivity can be calculated by:

$$q' = \frac{\sigma\cdot\left(T_{\mathrm{a}}^4 - T_{\mathrm{b}}^4\right)}{\frac{1-\varepsilon}{A_{\mathrm{a}}\cdot\varepsilon} + \frac{1}{A_{\mathrm{a}}\cdot F_{\mathrm{a-b}}} + \frac{1-\varepsilon}{A_{\mathrm{b}}\cdot\varepsilon}} \tag{13}$$

Where:

q': Heat flux per unit length in $\mathrm{W\cdot m^{-1}}$

σ: Stefan-Boltzmann constant, it is:

$$\sigma \approx 5.67\cdot 10^{-8}\,\frac{\mathrm{W}}{\mathrm{m^2\cdot K^4}} \tag{14}$$

$T_{\mathrm{a}}, T_{\mathrm{b}}$: Surface temperatures in K

$A_{\mathrm{a}}, A_{\mathrm{b}}$: Surface areas per unit length in $\mathrm{m^2\cdot m^{-1}}$

$F_{\mathrm{a-b}}$: Geometric view factor between the two bodies

ε: Emissivity of the surface

For two coaxial cylinders, it is:

$$F_{\mathrm{a-b}} = 1 \tag{15}$$

And the emissivity of aluminium is assumed to be:

$$\varepsilon = 0.1 \tag{16}$$

Inserting the radii and regrouping equation (13) yields:

$$R_{\mathrm{th,iso,rad}} = 5.52\cdot 10^{8}\,\frac{\mathrm{m\cdot K^4}}{\mathrm{W}}\cdot\frac{T_{\mathrm{a}} - T_{\mathrm{b}}}{T_{\mathrm{a}}^4 - T_{\mathrm{b}}^4} \tag{17}$$

3.3.2 Heat transfer by convection

With respect to the heat transfer by convection, [4] gives an extensive comparison between three formulas, found in [5], [6] and [7]. **Figure 3** displays the calculated heat flux per unit length inside the GIL as a function of relevant temperature differences between the inner conductor and the outer enclosure. In order to neglect the influence of the actual gas mixture inside the GIL, the insulation is assumed to consist of nitrogen only at 7 bar absolute pressure for this comparison. Gases with higher density like SF_6 would improve the total heat flux.

The results are in line with the findings in [4], with the expression from [7] underestimating the transferred heat, whereas between the expression from [5] or [6] and the numerical simulation, a relatively good accordance can be stated. The impact of the illustrated differences on the ampacity rating will be further highlighted in chapter 3.6.

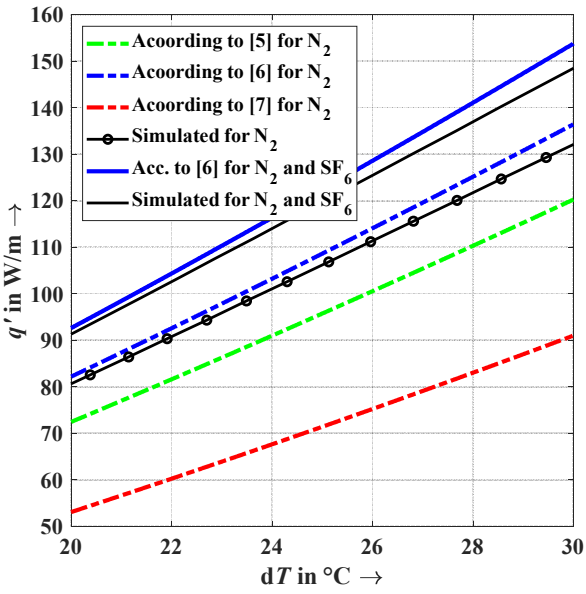

Figure 3 Calculated and simulated heat flux per unit length (q') by convection inside the GIL as a function of relevant temperature differences (dT) between inner conductor and enclosure; for N_2 and a mixture of 80% N_2 and 20% SF_6.

For the final simulations, a mixture of 80% N_2 and 20% SF_6 was assumed, as frequently used in GIL [8]. With respect to the simulations, the effect of SF_6 was incorporated by adjusting the thermal conductivity of pure nitrogen, as no sufficient information about the temperature and pressure dependent properties of SF_6 was available. The result in comparison to the calculations based on [6] is equally shown in Figure 3.

Inserting the characteristics of the geometry as well as the gas into the formulation of [6] leads to:

$$R_{\mathrm{th,iso,conv}} = \frac{0.45}{(T_{\mathrm{a}} - T_{\mathrm{b}})^{0.25}}\,\frac{\mathrm{m\cdot K^{1.25}}}{\mathrm{W}} \tag{18}$$

3.3.3 Total thermal resistance of the GIL

The total thermal resistance of the GIL is finally computed by:

$$R_{\mathrm{th,GIL}} = \frac{R_{\mathrm{th,iso,conv}}\cdot R_{\mathrm{th,iso,rad}}}{R_{\mathrm{th,iso,conv}} + R_{\mathrm{th,iso,rad}}} + R_{\mathrm{th,jac,GIL}} \tag{19}$$

Where:

$$R_{\mathrm{th,jac,GIL}} = \frac{1}{2\pi\cdot\lambda_{\mathrm{HDPE}}}\cdot\ln\left(\frac{r_{\mathrm{GIL}}}{r_{\mathrm{jac,GIL}}}\right) = 0.013\,\frac{\mathrm{K\cdot m}}{\mathrm{W}} \tag{20}$$

However, as it was demonstrated in sections 3.3.1 and 3.3.2, the thermal resistances of the insulation are highly dependent on the temperature difference and the heat flux. As a consequence, it can only be determined iteratively by computing the total system. When evaluating the final solution, $R_{\mathrm{th,GIL}}$ can be determined as:

$$R_{\mathrm{th,GIL}} \approx 0.20\,\frac{\mathrm{K\cdot m}}{\mathrm{W}} \tag{21}$$

It has thus half the value of the cable's thermal resistance.

3.4 Thermal resistance of the bedding

Assuming the ground surface to be an isothermal at reference temperature, the Kennelly-formula for the external resistance can be used [9]. In this case, it is:

$$R_{\mathrm{th,soil}} = \frac{1}{2\pi\lambda_{\mathrm{soil}}} \ln\left(\frac{y_0}{r_\mathrm{o}} + \sqrt{\left(\frac{y_0}{r_\mathrm{o}}\right)^2 - 1}\right) \tag{22}$$

Where:

r_o: r_c for $R_{\mathrm{th,soil,c}}$ or r_{GIL} for $R_{\mathrm{th,soil,GIL}}$

3.5 Mutual heating of the systems

Finally, the thermal interference between the two poles must be taken into account. This can be done by placing a line source (as well as its image to respect the Dirichlet condition on the ground surface) so that the cable outer surface is an isothermal. Hence:

$$\mathrm{d}T_{\mathrm{ad}} = \frac{q'}{4\pi\lambda_{\mathrm{soil}}} \ln\left[\frac{(d+2\cdot r_\mathrm{o})^2+(y_0-k)^2}{(d+2\cdot r_\mathrm{o})^2+(y_0+k)^2}\right] \tag{23}$$

With:

$$k = \sqrt{y_0 - r_\mathrm{o}} \tag{24}$$

The heat injection is chosen in such a way that the temperature on the outer jacket of the cable or GIL equals the values found by the calculations of one pole alone. Therefore, it is:

$$q' = \mathrm{d}T_\mathrm{o} \cdot \frac{2\pi\lambda}{\ln\left(\frac{r_\mathrm{o}-y_0-k}{r_\mathrm{o}-y_0+k}\right)} \tag{25}$$

With:

$\mathrm{d}T_\mathrm{o}$: Temperature rise on the outer surface of the cable or GIL for one single cable or GIL

3.6 Validation of the results

Comparing the results from equation (2) and the numerical results, it is not surprising that with respect to the HVDC cable systems, the differences are negligible. The outcome of the numerical calculations – assuming a maximum conductor temperature of 70 °C at a reference temperature of 20 °C – is $I_{\mathrm{max,cab}} = 2180$ A per pole, whereas by following the analytical procedure, the result is $I_{\mathrm{max,cab}} = 2200$ A. The difference is only due to the approximate calculations of the mutual heating, explained in section 3.5.

With respect to the gas-insulated system, the conductor temperature as a function of the pole current is drawn in **Figure 4** for different calculations of $R_{\mathrm{th,iso,conv.}}$ It can be stated that the differences illustrated in Figure 3 translate into considerable differences in temperature between the mentioned methods. However, considering a maximum allowed conductor temperature of 105 °C, the results are between 4900 A and 5130 A, i.e. the vary within a range of only 5 %.

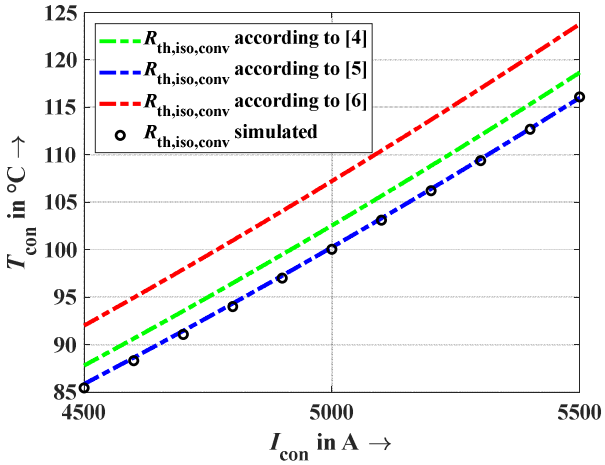

Figure 4 Calculated (according to the presented equations) and simulated (with the help of a numerical tool) GIL - conductor temperature (T_{con}) as a function of the conductor current (I_{con}) for different formulations of the thermal resistance due to convection between the inner conductor and the enclosure.

3.7 Technology comparison

In order to investigate the differences between the ratings of the cable and the GIL, **Table 6** shows relevant factors of influence and results, by which the mentioned ratings can be evaluated. It must be pointed out that for this consideration the conductor temperature is the target value; all other values are a result of the calculation.

Table 6 Factors of influence and results of the ampacity calculation under the assumption of a homogenous bedding of $\boldsymbol{\lambda_{\mathrm{soil}}}$= 1 W·m^{-1}·K^{-1}. T_o is the temperature on the surface of the outer jacket

	Cable	GIL
T_{con} in °C	70	105
$R_{\mathrm{th,cab}}$ or $R_{\mathrm{th,GIL}}$ in m·K·W^{-1}	0.40	0.20
$R_{\mathrm{th,soil}}$ m·K·W^{-1}	0.59	0.34
T_o in °C	60	80
$\mathrm{d}T_{\mathrm{ad}}$ in °C	8	17
P'_{max} in W·m^{-1}	41	125
I_{max} in A	2180	5155
$P_{\mathrm{el,max}}$ in GW	2.40	5.67

One major advantage of the HVDC GIL against the HVDC cable (in terms of the ampacity rating) is the higher admissible conductor temperature T_{con}, as well as its higher enclosure temperature T_o. Assuming a reference temperature of 20 °C, the allowed temperature difference between the conductor and the soil surface is 70 % higher for the GIL than for the HVDC cable. Furthermore, the thermal resistances R_{th} of the GIL and its bedding are equally smaller due to its larger diameter. Although the thermal interference between the two poles is higher for the gas-insulated system than between the two cables, the admissible heat dissipation P'_{max} is three times larger for GIL. Together with the lower conductor resistance, this leads to a maximum power transmission of 5.67 GW for GIL, comparing to 2.40 GW for the HVDC cables.

4 Transmission capacity for HVDC corridors in practice

In contrast to the calculations in chapter 3, a realistic ampacity calculation must take into account multiple restrictions or boundary constraints. The impact of the following scenarios shall be examined:

I. Consideration of the soil drying out: All soils are implemented according to the two-zone model with a thermal conductivity of the wet soil of 1 $Wm^{-1}K^{-1}$, of the dry soil of 0.4 $Wm^{-1}K^{-1}$, and a critical temperature rise (i.e. the temperature at which drying out appears) of 15 K.

II. Use of thermally stabilized bedding and backfill material: Only the natural soil is subjected to a drying out, while for the bedding and backfill material, it is:

$$\lambda_{\mathrm{bed}} = 1.5\ \frac{\mathrm{W}}{\mathrm{m{\cdot}K}} = \mathrm{const.} \tag{26}$$

$$\lambda_{\mathrm{back}} = 1.25\ \frac{\mathrm{W}}{\mathrm{m{\cdot}K}} = \mathrm{const.} \tag{27}$$

III. Restriction of the maximum soil temperature: To safely avoid denaturation of proteins [10], a maximum temperature within the natural soil of 47.5 °C could be imposed in the future by environmental regulations. Hence, not the maximum conductor temperature is the decisive criterion, but the temperature at the frontline between the thermally stabilized bedding and the natural soil.

IV. Use of cable protection pipes: Due to requirements of the laying process, large parts of future HVDC-cables may have to be laid inside air filled protection pipes. This introduces a supplementary thermal resistance, which – by leaving the spacing between the cables unchanged – results in a reduction of the current carrying capacity.

V. Higher admissible cable temperature: New developments have led to HVDC cables with T_{max} = 90 °C [11].

From the multitude of possible combinations of scenarios, a selection of the results are given in **Table 7**. For all calculations, the reference temperature is 20 °C.

Scenario I considers a direct laying into a soil with poor thermal characteristics, which represents a very conservative, if not unrealistic scenario. It can be stated that the resulting ampacity ratings diverge by about 20 % from the findings in chapter 3. A more realistic scenario is assumed by considering thermally stabilized bedding and backfill. However, with respect to scenario III, it is worth pointing out that a purely technical perspective may be insufficient, when dimensioning underground power transmission: If such restriction is in place, the advantage of a higher maximum conductor temperature (for the GIL or the improved cable) is no longer valid.

And it should also be mentioned that there are more possibilities to improve the rating that are not included in this evaluation: E.g., the spacing between the poles as well as the dimensions of the trench and the backfill could be enlarged.

Table 7 Simulated maximum currents and transport capacity taking into account the mentioned scenarios.

	I_{max} in A		$P_{\mathrm{el,max}}$ in GW	
Scenario	**Cable**	**GIL**	**Cable**	**GIL**
Chapter 3	2180	5155	2.40	5.67
I.	1850	4000	2.04	4.40
I. - II.	2320	5400	2.55	5.94
I. - III.	2250	3900	2.48	4.29
I. - IV.	2110	-	2.32	-
I. - V.	2200	-	2.42	-
I. - II., IV - V.	2500	-	2.75	-

5 Comparison of costs

Finally, the derived ampacity ratings are now put into relation to the costs. In general, it must be distinguished between the costs of investment and operation, where the first can be further split up into the costs of construction and costs of equipment. With respect to the cost of operation, not just the losses but also the reliability must be taken into consideration. As no reliable data in this regard is accessible at this point, the following considerations will focus on the costs of investment only.

With respect to the values from Table 7, it can be stated that for transmission capacities up to 2.5 GW, one bipolar cable system can be considered. For larger transmission capacities, two systems must be taken into account. GIL will operate in the range of 5 GW with one bipolar system. The n-1 criterion is disregarded in both cases.

5.1 Costs of construction

Under an abstract perspective, the cost of construction can be assumed as the sum of the costs of the backfill material and the general costs of the trench. The first can be assumed proportional to the volume of bedding material, whereas the latter is considered to be proportional to the total volume of the trench. Hence:

$$C_{\mathrm{con}} \sim A \cdot V_{\mathrm{bed}} + B \cdot V_{\mathrm{trench}} \tag{28}$$

With:

C_{con}: Cost of construction in €·m^{-1}

$V_{\mathrm{bed}}, V_{\mathrm{trench}}$: Volume of the backfill material (total trench) per unit length in m^2

A, B: Constants in €·m^{-3}

As the same thermal properties of the bedding and backfill material have been assumed in the preceding calculations, the constants A and B are considered to be the same for the cable and the GIL. Hence, with the help of the volumes given in Table 3 the ratio between the costs of construction for cable and GIL can be given as a function of the ratio between the two constants. This is done for one and two cable systems (i.e. for a maximum transmission capacity of about 2.5 GW and 5 GW) in **Figure 5**. In practice, there may exist large deviations of the ratio A/B. E.g. at construction in a rural surrounding with unused soil, the soil might be directly reused for the backfill, which leads to a low value of the trench costs ($A/B > 1$). Construction in urban areas may result in high

additional costs, e.g. because of disposal of the excavation and the insertion of new material ($A/B < 1$).

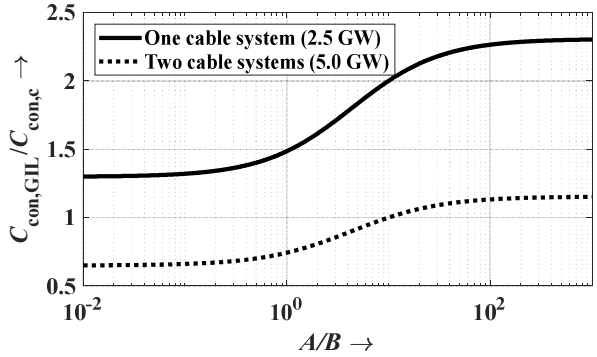

Figure 5 Ratio between the cost of construction (C_{con}) for a GIL and a cable system depending on the ratio of the cost coefficients A and B for one cable system (transmission capacity up to 2.5 GW) and two cable systems in separate trenches (up to 5 GW) in logarithmic scale.

As it can be seen, the construction costs for a GIL are always higher if a transmission capacity of 2.5 GW is envisaged (hence, only one cable system is needed). If two cable systems are needed, this is only the case for a ratio of the two coefficients of $A/B > 10$, as in this case, the higher volume of bedding material in the case of a GIL exceeds the impact of the higher overall trench volume for two cable systems.

5.2 Costs of equipment

Regarding the cost of the equipment, it is assumed that they can be considered as the sum of the material costs and supplementary costs (the cost of production, transportation, laying-costs as well as equipment and other overhead-costs). Hence:

$$C_{\mathrm{equip}} = C_{\mathrm{mat}} + \mathrm{d}C_{\mathrm{sup}} \tag{29}$$

Where:

C_{equip}: Total cost of equipment in €·m^{-1}

C_{mat}: Cost of material (copper, XLPE and HD-PE for cables, aluminium, SF_6 and HD-PE for GILs) in €·m^{-1}

$\mathrm{d}C_{\mathrm{sup}}$: Supplementary costs (subsuming all other costs rather than C_{mat})

Assuming common market prices, the material costs for one system (i.e. two poles) can be approximated to:

$$C_{\mathrm{mat,c}} = 325\,\frac{€}{\mathrm{m}} \tag{30}$$

$$C_{\mathrm{mat,GIL}} = 300\,\frac{€}{\mathrm{m}} \tag{31}$$

where about 70 % are due to the costs of the conductive materials. Hence, the material costs are very close to each other, with the difference in the total cost of equipment largely due to $\mathrm{d}C_{\mathrm{sup}}$.

5.3 Total investment costs

Finally, the ratio of the total investment cost can be written as:

$$r = \frac{C_{\mathrm{con,GIL}} + C_{\mathrm{mat,GIL}} + \mathrm{d}C_{\mathrm{sup,GIL}}}{C_{\mathrm{con,c}} + C_{\mathrm{mat,c}} + \mathrm{d}C_{\mathrm{sup,c}}} \tag{32}$$

By using the approximation that 40% of the project costs of a GIL are due to the construction [8], one may write:

$$C_{\mathrm{con,GIL}} = \frac{2}{3} \cdot \left(C_{\mathrm{mat,GIL}} + \mathrm{d}C_{\mathrm{sup,GIL}}\right) \tag{33}$$

By further using the results from section 5.1, i.e.:

$$C_{\mathrm{con,GIL}} = f\left({}^{A}/_{B}\right) \cdot C_{\mathrm{con,c}} \tag{34}$$

Equation (32) can be used in order to derive the costs $\mathrm{d}C_{\mathrm{sup,cab}}$ as a function of $\mathrm{d}C_{\mathrm{sup,GIL}}$ as well as the ratio r. For equal costs of investment ($r = 1$) and one cable system, this is done in **Figure 6**, top, for two prominent values of A/B. Furthermore, the ratio in equation (33) is varied: For the mentioned 40 %, the values are shown in green. If the construction costs of the GIL amount to 20 % or 60 % of the total costs, the red or blue curves can be used, respectively. Such variations may occur in practice, because costs of construction sites may significantly change, e.g. because of groundwater level control, disposal of contaminated soil or high costs due to environmental regulations.

Hence, the first graph in Figure 6 can be read as following: In the case that the cost of the specialized bedding is predominant in the cost of construction ($A/B \geq 100$) and the ratio of the construction costs to the total costs of the GIL is 40 %, the supplementary costs of the cable can be 40 % higher than $\mathrm{d}C_{\mathrm{sup,GIL}}$, if the latter amounts to 1000 €·m^{-1}. The curve increases for smaller values of $\mathrm{d}C_{\mathrm{sup,GIL}}$, or higher portions of the construction costs for the GIL, as the larger volume of the specialized bedding material gains influence.

If the costs of construction are only to a small amount influenced by the costs of the backfill material ($A/B \leq 1$), the possible cost advantage of the cable with respect to the GIL becomes less pronounced, as it can be seen by comparing the dotted to the full curves. Nonetheless, the required values of $\mathrm{d}C_{\mathrm{sup,c}}$ to obtain equal investment costs will surely be met. Supplementary costs for GIL installations are estimated to be higher, because a high number of modules are welded at site, while larger length of cable systems are produced and tested in the factory. A higher cost efficiency of one cable system in comparison to one GIL system is therefore very likely.

The situation is different, if two cable systems are needed to obtain the targeted transmission capacity. In analogy to the graph discussed above, Figure 6, bottom, shows the equivalent curves for transmission capacities higher than 2.5 GW. Due to the slightly higher costs of material as well as construction costs of the cable, the cost factor $\mathrm{d}C_{\mathrm{sup,c}}$ would have to be even negative for values of $\mathrm{d}C_{\mathrm{sup,c}} < 1000$ €/m in order to reach equal costs of investment. GIL would therefore be the more cost efficient solution in this area.

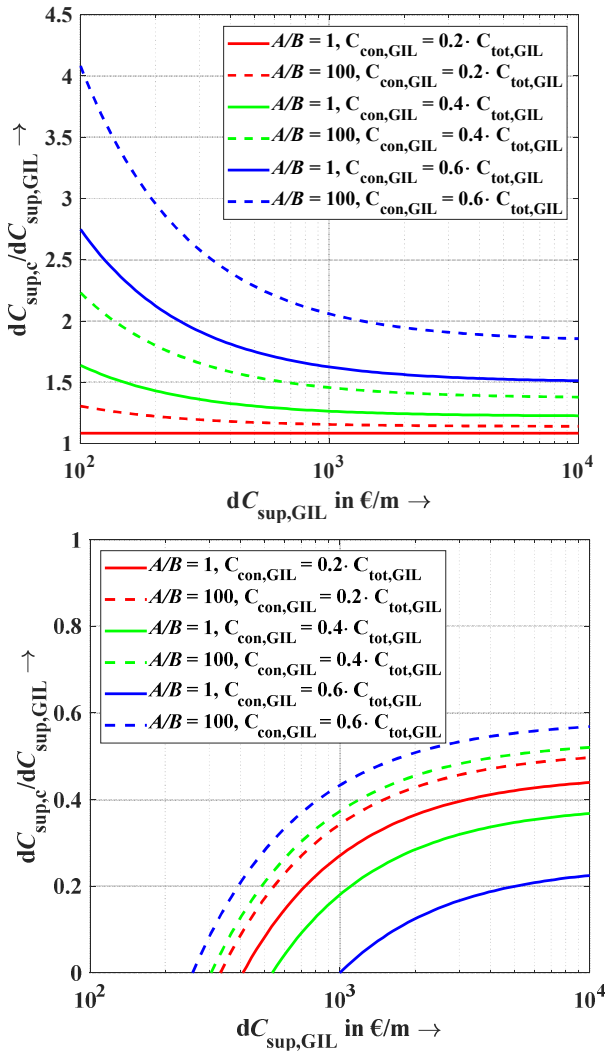

Figure 6 Relative supplementary costs of a cable ($dC_{sup,cab}$) as a function of the supplementary costs of a GIL ($dC_{sup,GIL}$) for an equal cost of investment ($r = 1$) and to values of A/B as well as three ratios between the cost of construction and the total costs of the GIL. Top: Transmission capacity up to 2.5 GW (one cable system); Bottom: Transmission capacity up to 5 GW (two cable systems).

Conclusion

Resuming the present contribution, it is worth pointing out that it contains the major fundamental aspects of a comparison between the ampacity ratings as well as investment costs of HVDC cable systems and HVDC-GILs.

With respect to the first aspect, it is demonstrated that the higher transmission capacity of the GIL is due to three factors: the lower conductor resistance, the higher admissible temperature as well as the lower overall thermal resistance between the conductor and the ground surface.

Furthermore, practical restrictions of the ampacity ratings are taken into consideration. This includes the incorporation of a possible soil drying out, the use of thermally stabilized backfill materials or environmental restrictions regarding the maximum soil temperature. As it is shown, the latter may severely limit the advantage of the higher admissible conductor temperature of the GIL (or novel HVDC cables with a maximum conductor temperature of 90 °C).

Finally, the costs of investments are compared using a general approach that covers a large variety of possible ranges of costs, the main statement is that HVDC GIL technology becomes competitive for transmission capacities higher than 2.5 GW, i.e. when two or more cable systems are needed instead of only one GIL system.

With respect to future work, the inclusion of the cost of operation into the presented evaluation may be the most prominent gap to close. Furthermore, the role of a third pole as a metallic return or to ensure the n-1 safety is worth considering.

6 Bibliography

[1] CIGRE Working Group D1.56: CIGRE TECHNICAL BROCHURE n°794 “Field grading in electrical insulation systems”, 2020

[2] M. Hallas et al. “CIGRE Prototype Installation Test for Gas-Insulated DC Systems – Testing a Gas-Insulated DC Transmission Line (DC-GIL) for ±550 kV and 5000 A under Real Service Conditions” in CIGRE Session 48, Paris, Report D1-107, 23-28 August 2020

[3] CIGRE Joint Working Group B3/B1.27: CIGRE TECHNICAL BROCHURE n°639 “Factors for Investment Decision GIL vs. Cables for AC Transmission”, 2015

[4] CIGRE Joint Working Group 23/21/33-15: CIGRE TECHNICAL BROCHURE n°218 „Gas Insulated Transmission Lines (GIL)“, 2003

[5] Itaka, K. Araki, T. and Hara, T.: ‘Heat transfer characteristics of gas spacer cables, IEEE Transactions on Power Apparatus and Systems’, Vol. PAS-97, No. 5, Sept/Oct 1978

[6] Minaguchi, D. Ginno, M. Itaka, K. Furukawa, H. Ninomiya, K. and Hayashi, T.: ‘Heat Transfer Characteristics of Gas-Insulated Transmission Lines’, IEEE 85 SM 301-7

[7] Electra No. 125 ‘Calculation of the Continuous Rating of Three Core, Rigid Type, Compressed Gas Insulated Cables in Still Air and Buried.” (1989) pp 104-111

[8] Koch, H.: GIL – Gas-Insulated Transmission Lines. John Wiley & Sons, Chichester, 2012

[9] IEC Standard 60287-2-1 2006, Electric cables – calculation of the current rating. Part 2.1

[10] Horton, H. R. et al.: Principles of Biochemistry. Third edition, Pearson Education by Prentice-Hall, Inc., Upper Saddle River, pp. 104

[11] Igi, T. et al.: Qualification, installation and commissioning of world’s first DC 400 kV XLPE cable system. 10th international conference on unsulated power cables, Jicable 19, June 23rd - 27th, Versailles, France